II. CVD GROWTH OF 3C-SiC ON Si SUBSTRATES

1. Introduction

In this investigation, 3C-SiC was grown on Si substrates by the combination of the carbonization and the CVD growth. First in this chapter, the apparatus and the procedures for growth are introduced. Next, the characterization of carbonized layers and grown layers and the optimization of various conditions concerning growth are mentioned. The structure of the carbonized layers is discussed based on the characterization by various methods. Variations of crystallinity due to flow rates of source gases and film thickness are described. Through the RHEED observation of grown layers on various faces of Si substrates, a model of a carbonization mechanism is brought up. Finally attempts for lowering of growth temperature using C_2H_2 are also mentioned. These subjects were investigated with the aim of obtaining "good crystals" for the fabrication of electronic devices.

2. CVD apparatus and growth procedures

(CVD apparatus)

Figure 1 shows a schematic diagram of a CVD growth system. The appearances of a reaction tube and mass-flow-control units are shown in Figs.2 and 3. The epitaxial growth of 3C-SiC by CVD was carried out in a horizontally set quartz reaction-tube at ordinary atmospheric pressure. A cross section of the reaction tube was a circle of 5cm in diameter and it had a water cooling jacket. A carrier gas was refined hydorgen(H_2) by a purifier and its typical flow rate and linear velocity were 3 SLM and 5 cm/s, respectively. Source gases were, hereafter if not specially annotated, silane(SiH_4) and propane(C_3H_8). Methane(CH_4) and acetylene(C_2H_2) were also used for carbon sources. Diborane(B_2H_6)

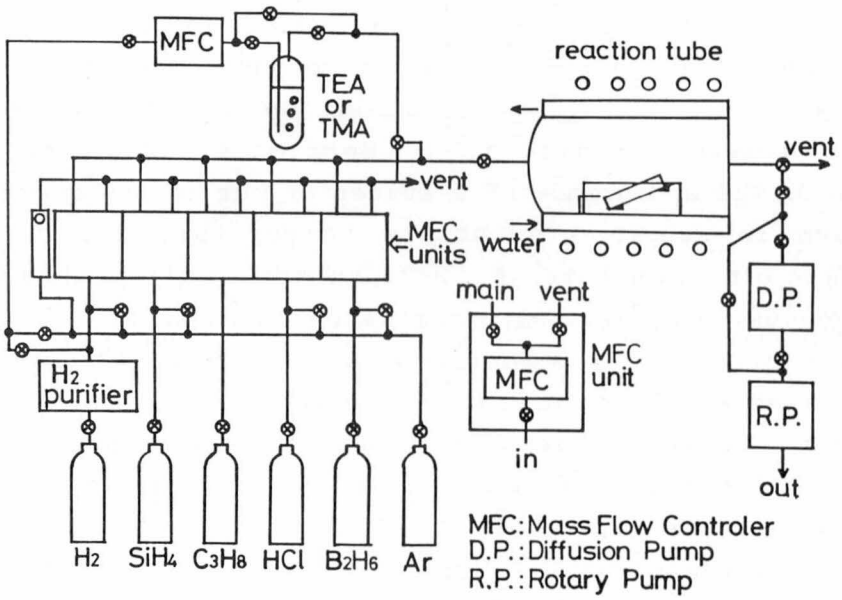

Fig.1 Schematic diagram of CVD growth system.

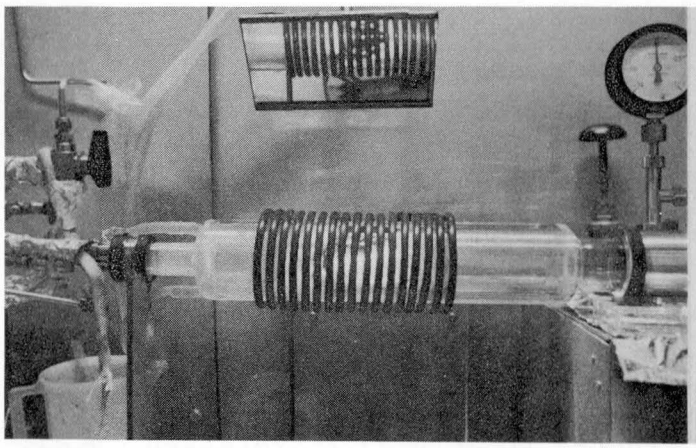

Fig.2 Reaction tube for CVD growth.

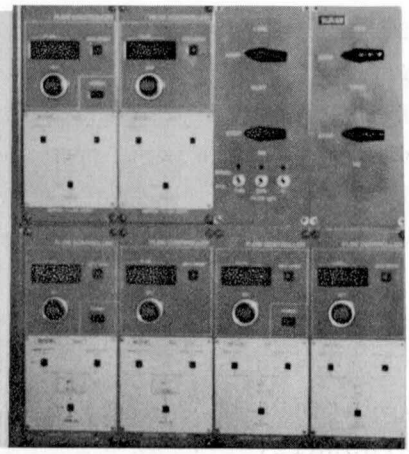

Fig.3 MFC(mass-flow controller) system.

and organic aluminum were used for doping. Source gases and B_2H_6 were diluted with H_2. The used organic aluminum is liquid at room temperature and they were introduced by a bubbling method. Hydrogen chloride(HCl) was used for etching of substrates.

A substrate was put on a graphite susceptor coated with SiC and they were heated by RF induction. The quality of the coating affects growth conditions. In Section 4-1 this problem is mentioned. The appearance of a susceptor set in its quartz holder is shown in Fig.4. A substrate temperature was decided by measuring a temperature of a hole formed at the backside of the susceptor using an optical pyrometer.

The susceptor was inclined at an angle of 10° towards the upper stream as shown in Fig.4 in order to improve the uniformity of film thickness. Figures 5(a) and (b) represent the variation of film thickness as a function of the distance from the front edge of a substrate for horizontally set and inclined susceptors, respectively. The linear velocity of a carrier gas was increased from 0.85cm/s to 5cm/s in the latter case by the increase of a flow rate of a H_2 carrier gas and a modification of the susceptor holder. When the susceptor was set horizontally and linear velocity was low, the film thickness at the front edge was 5 times greater than that at the back edge as shown in Fig.5(a). The uniformity of the film thickness was much improved as shown in Fig.5(b) by the inclination and the increase of the linear velocity. The combinations of an inclined susceptor and the low linear velocity or a horizontal susceptor and the high linear velocity did not give such improvement as shown in Fig.5(b).

These results are explained by "a stagnant layer model" brought up by Everstyen et al.[1]. Around an object in a moving fluid with low viscosity such as water or the air, there is a layer named the boundary layer where the velocity of the fluid gradually decreases and reaches to zero[2]. Everstyen et al. used a simplified model for the boundary layer, namely, the stagnant layer where the velocity of the fluid is zero and the temperature of the fluid is constant in order to estimate the growth rate of a crystal in CVD system. When this model can be

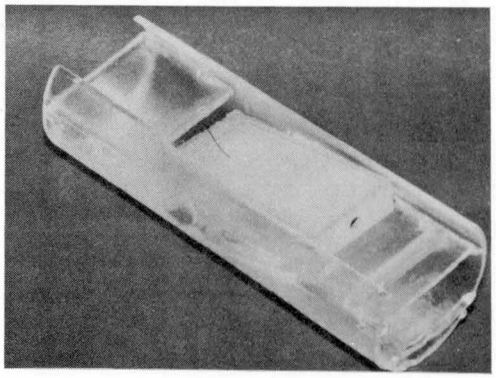

Fig.4 Susceptor and its quartz holder.

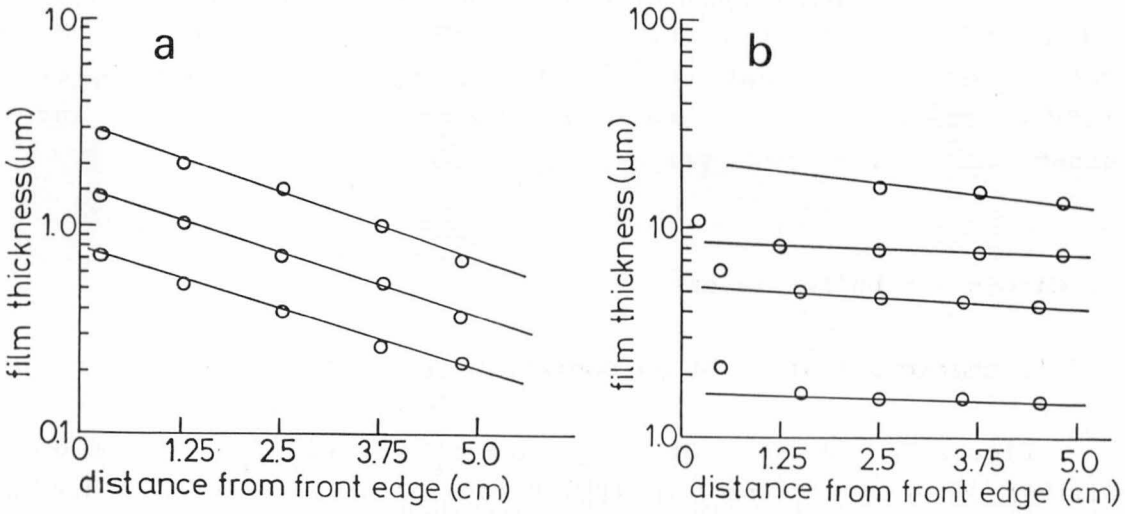

Fig.5 Relationship between film thickness and the distance from the front edge of a substrate. Susceptors were set (a)horizontally and (b)tilted at 10°.

applied, similar to Fig.5(a), film thickness changes proportional to the reciprocal of an exponential function of the distance from the front edge of a sample. Through calculation and experiments they found that the uniformity of the film thickness was improved by the inclination of substrates and the high linear velocity of a carrier gas.

In the case of this investigation, the further increase of the linear velocity to 10cm/sec showed no meaningful improvement of the uniformity. Therefore, by taking economy into consideration the linear velocity was fixed to 5cm/sec.

(Growth procedure)

The temperature program of CVD growth procedure is shown in Fig.6. The crystal growth procedure consists of three processes. The first process is etching of a Si substrate by HCl gas at 1180°C. The flow rates of HCl and H_2 for etching were 10sccm and 1SLM, respectively. The second step is carbonization of the Si substrate with C_3H_8 at 1360°C for 2min. The typical flow rate of C_3H_8 and H_2 during carbonization were 1.2sccm and 1SLM, respectively. The last is CVD growth with SiH_4 and C_3H_8 at 1350°C. The typical flow rate of SiH_4 and C_3H_8 was 0.3sccm and about 0.25sccm, respectively.

3. Carbonized buffer layers

3-1. Characterization of carbonized buffer layers

Figure 7 shows a RHEED pattern of a carbonized layer on Si(100). When conditions for the carbonization were optimized, a spot pattern of single crystalline 3C-SiC was obtained. There are three important parameters for the carbonization. They are time, temperature and flow rate of C_3H_8. If the conditions were far from the optimized situation, carbonized layers were polycrystalline as shown in Figs.8(a) and (b). The samples whose RHEED patterns are shown in Figs.8(a) and (b) were prepared

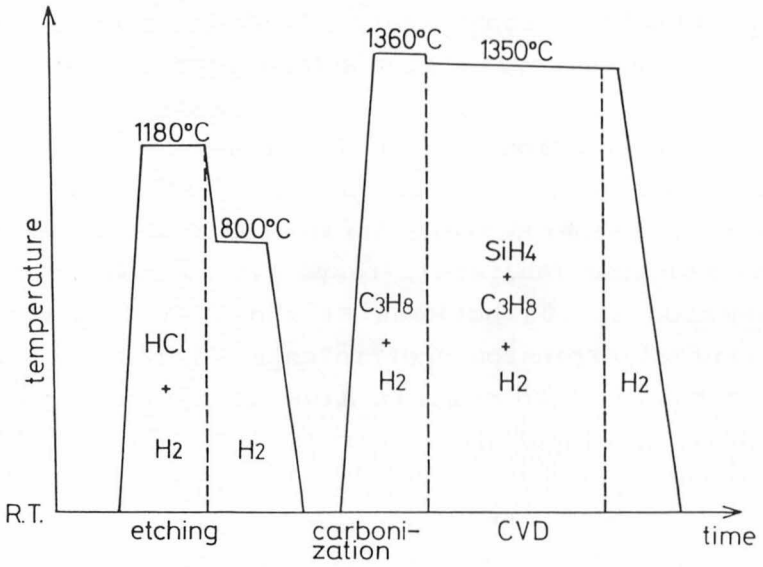

Fig.6 Temperature program of CVD growth procedures.

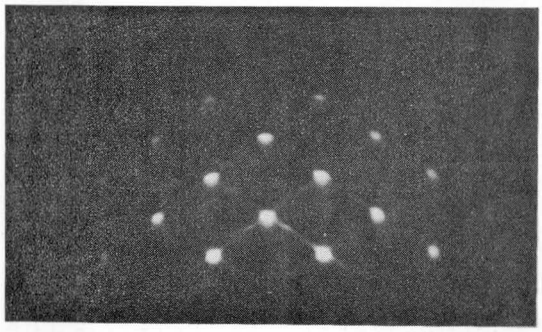

Fig.7 ‹011› azimuth RHEED pattern of a carbonized layer on Si(100) under the optimum condition.

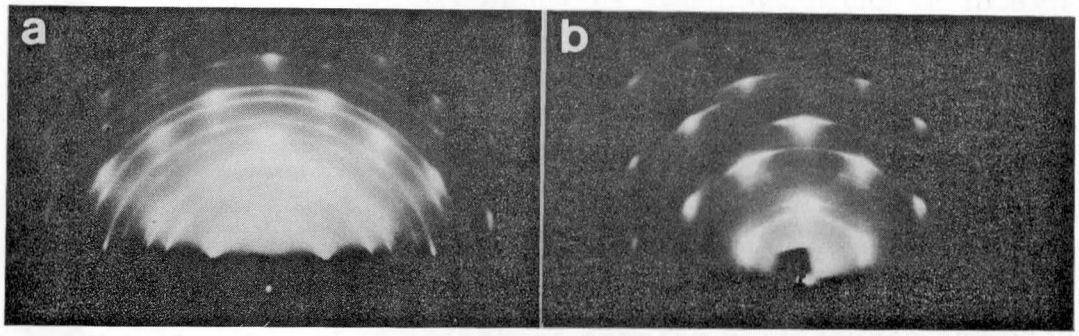

Fig.8 RHEED pattern of a carbonized layers on Si(100) under the off-optimum condition. (a)Too low flow rate of C_3H_8. (b) Too long carbonization time.

under the conditions of too low C_3H_8 flow rate and too long carbonization time[3], respectively. To obtain single-crystalline grown layers, single-crystalline carbonized buffer layers are preferable.

A careful observation of Fig. 7 reminds us of the existence of extra-spots and streaks spreading to $\langle 111 \rangle^*$. The extra-spots and streaks are considered to be originated from the existence of twinning and stacking faults[4], respectively. There is a large lattice mismatch of 20% between Si and 3C-SiC, and they have different thermal expansion coefficients. Therefore, thin grown layers are considered to contain high-density crystal defects induced by lattice mismatch and stress due to the difference in thermal expansion.

As mentioned above, the carbonized layers were confirmed to be single crystalline by RHEED observation. (In the strict sense, since twin-spots were slightly observed, they were not single crystalline. However, to avoid repeated troublesome explanations hereafter they are called to be simply "single crystalline".) However, the information obtained by RHEED observation was due to the area just close to the surface of samples. Because, the incidence angle of electron beams for RHEED observation is very low and the penetration depth of electron is not deep[5]. To discuss the mechanism of carbonization of Si, the information from the interface should be utilized.

An AES(Auger electron spectroscopy) depth profile of the carbonized layer on Si(100) is shown in Fig.9. The composition ratio of Si and C was close to 1.0 in the surface layer of 7nm in depth. Gradual change in the composition from SiC to Si was observed in the layer of 22nm in depth under the surface layer of SiC. Then the total thickness from the surface to the Si substrate was 29nm. These values were estimated using an etching rate of 3nm/min. Similar results were obtained for the carbonized layer on Si(111). Except for SiC, no crystalline compounds of $Si_xC_{1-x}(x<1)$ are known. Therefore, the existence of the layer where the composition changes gradually is hard to understand. Figure 10 shows a surface of a carbonized layer observed by a

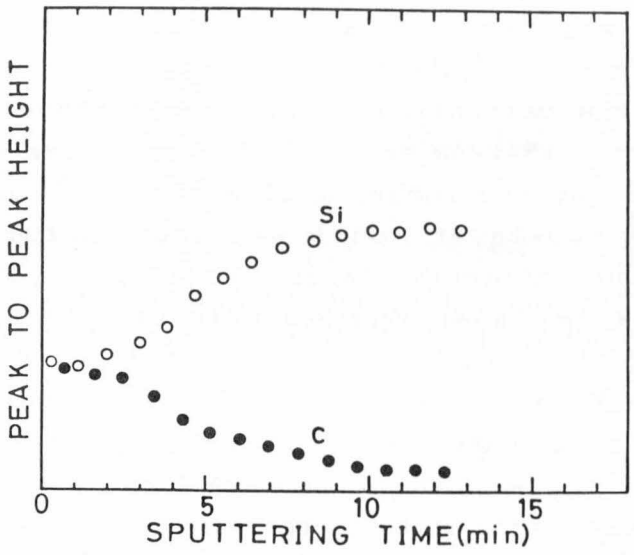

Fig.9 Auger electron spectroscopic depth profile of a carbonized buffer layer. An etching rate was about 3nm/min.

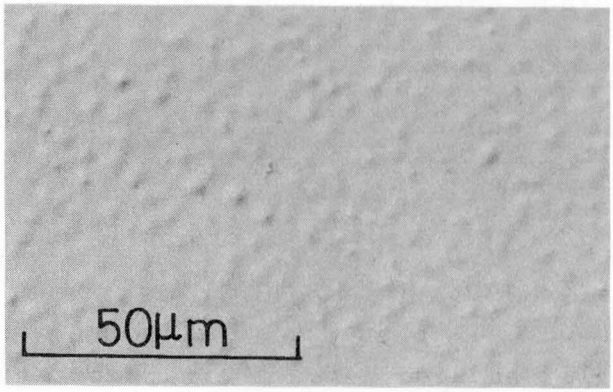

Fig.10 Nomarski microphotograph of the surface of a carbonized buffer layer on Si(100).

Nomarski microscope. Slight roughness was observed. If this roughness means that the thickness of SiC was not uniform because of island growth, there is a possibility that the difference in the thickness was observed as the gradual change of the composition around the interface in the depth profile of AES. Evaluation of the carbonized layer by ellipsometry gave a thickness of about 13-20nm and a refractive index of 2.7. This value of the refractive index is close to that of 3C-SiC of 2.64. A simple two-layer model was used to calculate the thickness and the refractive index of the film. If there are some intermediate layers, a multilayer model should be adopted[6].

TEM(transmission electron microscope) observation of the interface was carried out. A CVD grown layer on (100) with a thickness of 100nm was used. Figure 11(a) shows an XTEM(cross-sectional TEM) micrograph of the interface area observed from the ‹110› direction. Intervals of observed stripes correspond to the lattice spacing of (111) faces[7] and the stripes spread along one of the ‹111› directions forming an angle of 55° with the (100) face. Dark and light lines spread along another ‹111› direction and form 55° with the (100) face, which means the existence of plane defects. These plane defects are probably stacking faults or microtwins. The observed interface between SiC and Si was very sharp. Since the lattice spacings of the (111) faces differ in SiC and Si, all the stripes cannot be connected one by one. The enlarged picture of the interface area is shown in Fig.11(b). In this picture, one out of 4 or 5 lines of the stripes is disconnected at the interface. This interval of disconnections well agrees with the lattice mismatch of 20% between Si and 3C-SiC. Therefore, these disconnections indicate that periodically induced defects are important for lattice-mismatched epitaxial growth of 3C-SiC on Si(100).

3-2. Epitaxial relationship

Epitaxial relationship of substrates and heteroepitaxially

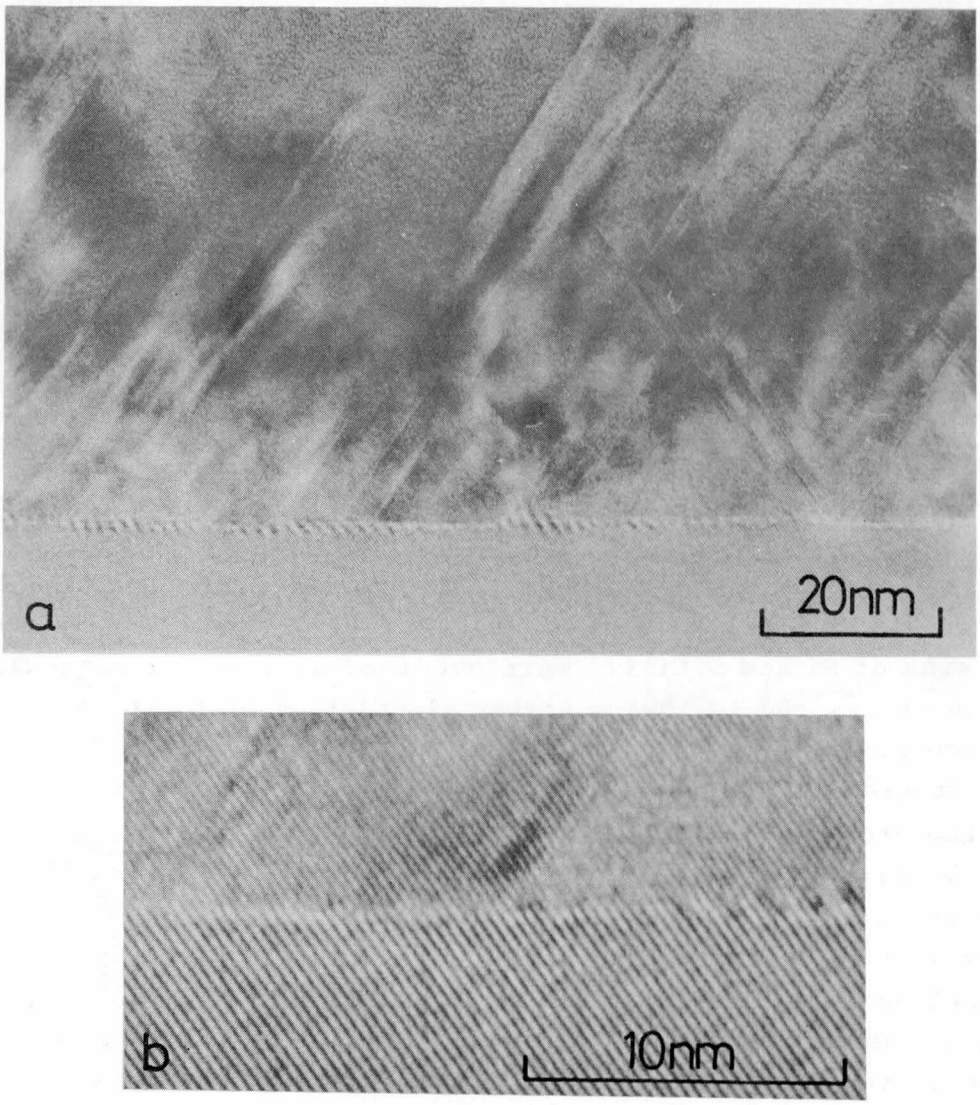

Fig.11 (a)XTEM photograph of a grown layer. (b) Magnified picture of (a).

grown layers can be identified utilizing etch pits, cleaving or a diffraction technique. In this subsection, a direct observation technique of the epitaxial relationship using electron diffraction is demonstrated. Electron beam was exposed to the edge of a sample as shown in Fig.12. The superposition of a transmission pattern from a substrate and a reflection pattern from a grown layer or a carbonized layer was obtained. Figs.13(a) and (b) show obtained patterns of grown layers on Si(100) and (111) substrates, respectively. Though CVD grown layers were used to take these patterns, the obtained epitaxial relationship was the same as that for carbonized layers. A schematic explanation of Fig.13 is shown in Fig.14. For a (100) substrate in Fig.14(a) superposition of <100> azimuth patterns of both Si and SiC(100) was obtained. In the previous sentence the index of a plane was given only to SiC, because transmission and reflection diffraction took place for a Si substrate and a SiC grown layer, respectively. In the case of a (111) substrate <211> azimuth patterns of Si and SiC(111) were obtained as shown in Fig14.(b). Conclusively, the following epitaxial relationships are obtained. For the growth on Si(100):

3C-SiC(100)//Si(100), 3C-SiC[011]//Si[011], and

for the growth on Si(111):

3C-SiC(111)//Si(111), 3C-SiC[$0\bar{1}1$]//Si[$0\bar{1}1$]

However, this conclusion does not describe the strict epitaxial relationship. Because, in spite that for 3C-SiC (111) and ($\bar{1}\bar{1}\bar{1}$) are not equal and for both Si and 3C-SiC [$0\bar{1}1$] and [$01\bar{1}$] are not equal, they are not distinguished here. To obtain the strict relationship utilization of other techniques may be necessary.

4. Crystallinity of grown layers

4-1. Dependence on Si/C ratio

Surface morphology and crystallinity of the grown layers are severely affected by the Si/C ratio(atomic ratio of Si and C in

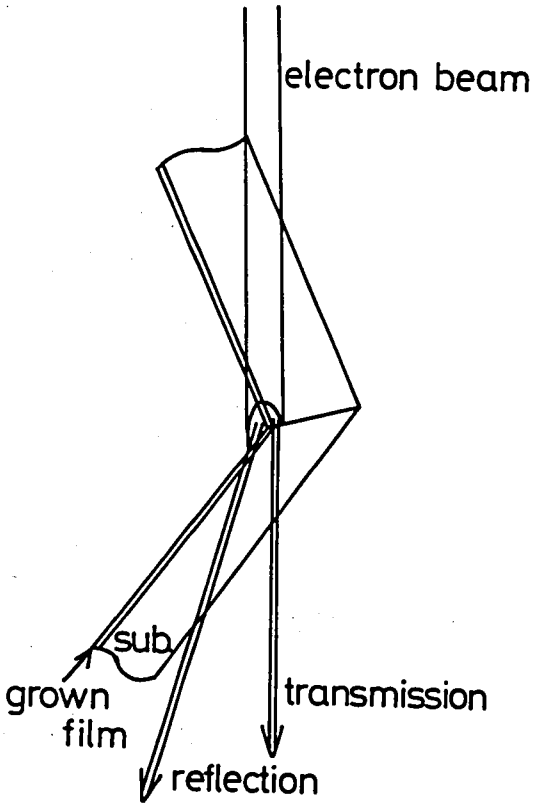

Fig.12 Electron beam which hits on the edge of a sample gives rise to both reflection and transmission diffraction.

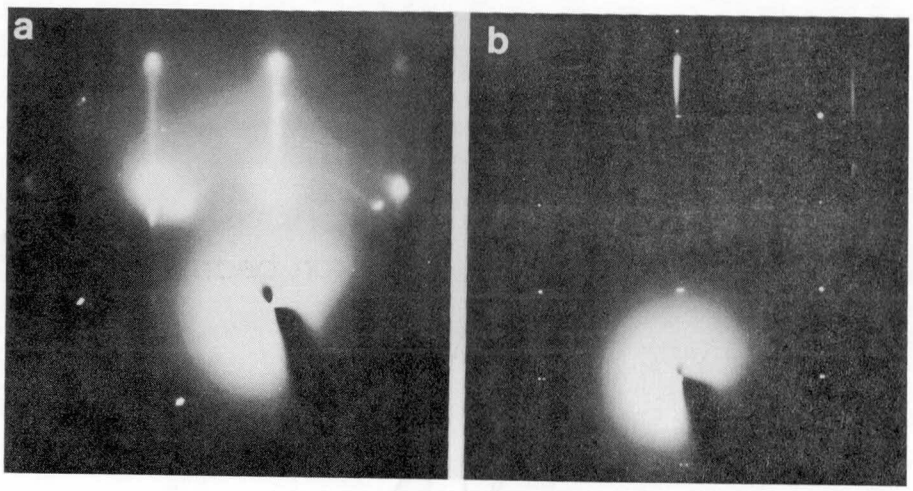

Fig.13 RHEED pattern of a SiC grown layer and the simultaneously obtained TED pattern of a Si substrate. (a) SiC(100) on Si(100). <010> azimuth. (b)SiC(111) on Si(111). <2$\bar{1}\bar{1}$> azimuth.

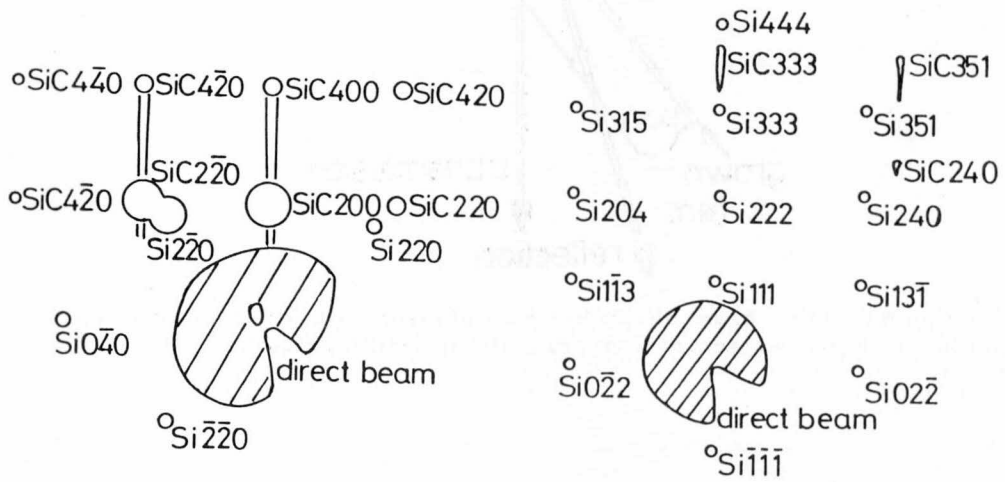

Fig.14 Schematic explanation of Fig.13. (a)SiC(100) on Si(100) and (b)SiC(111) on Si(111).

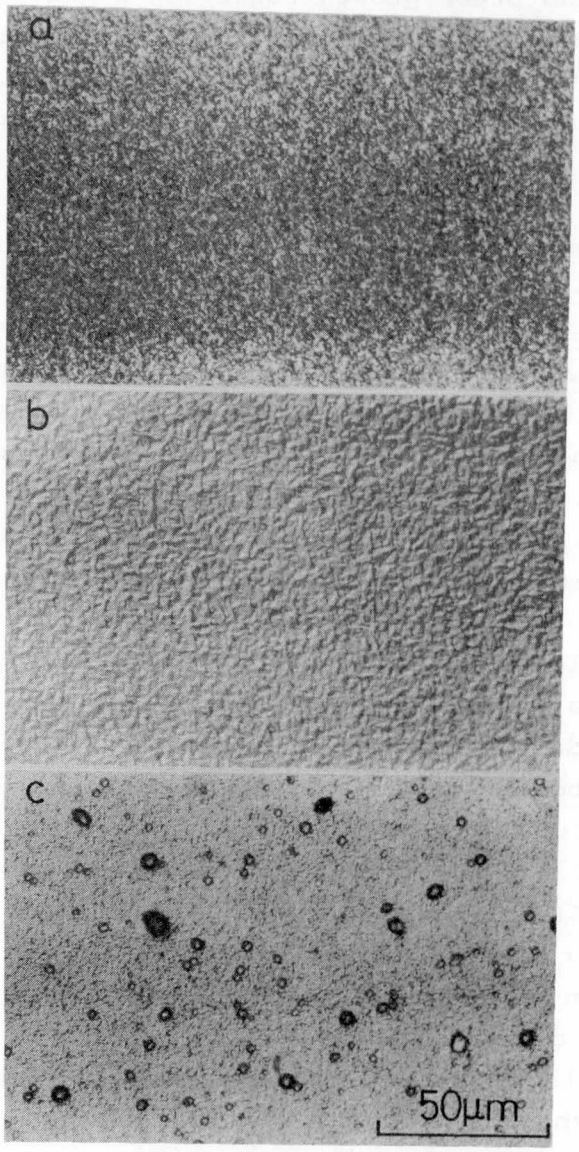

Fig.15 Si/C ratio dependence of surface morphology on Si(100). (a)Si-rich condition, Si/C=0.97, (b)moderate Si/C ratio, Si/C=0.34 and (c) C-rich condition, Si/C=0.27.

supplied source gases). Optimum Si/C ratio varies according to the change of a carbon source, growth temperature, orientations of substrates and other growth conditions. However, the feature of variation in surface morphology and crystallinity mentioned below were common to all cases. Here, examples of the grown layers on Si substrates oriented 4° off (100) towards (010) are shown. C_3H_8 was used for the carbon source and growth temperature was 1350°C.

The feature of the surface morphology was classified by the Si/C ratio into three types of Si-rich, moderate Si/C ratio and C-rich. Examples of the surface morphology are shown in Figs.15(a)-(c). Under the moderate Si/C ratio($Si/C \simeq 0.4$) condition, the surface of the grown layer became flattest. The surface was very rough and a random shape morphology was observed for the Si-rich condition ($Si/C >> 0.4$). For the C-rich condition ($Si/C << 0.4$), many needlelike crystals were observed. When CH_4 was used as the carbon source, a typical moderate Si/C ratio was about 0.15.

The crystals grown under the moderate Si/C ratio and the C-rich conditions gave streak and spot RHEED patterns of single crystalline 3C-SiC, respectively. Under the Si-rich condition, as the Si/C ratio became larger, the RHEED pattern gradually changed to a ring pattern of polycrystals. An example of the RHEED pattern of such a grown layer and its schematic explanation are shown in Figs.16(a) and (b), respectively. The polycrystals grown under the Si-rich condition contain both 3C-SiC and Si. Crystallization of excessively supplied Si was considered to obstruct single crystal growth of 3C-SiC.

The moderate Si/C ratio was severely affected by susceptor coating. Two types of susceptors were used. One was a graphite susceptor which was coated in the reaction tube using SiH_4 and C_3H_8 before growth. Hereafter susceptors of this kind are called in situ-coated susceptors. The other was a SiC-coated graphite susceptor which was produced for epitaxial growth of Si in factories. The coating of the latter susceptors looks denser by observation with the naked eyes. When the in situ-coated

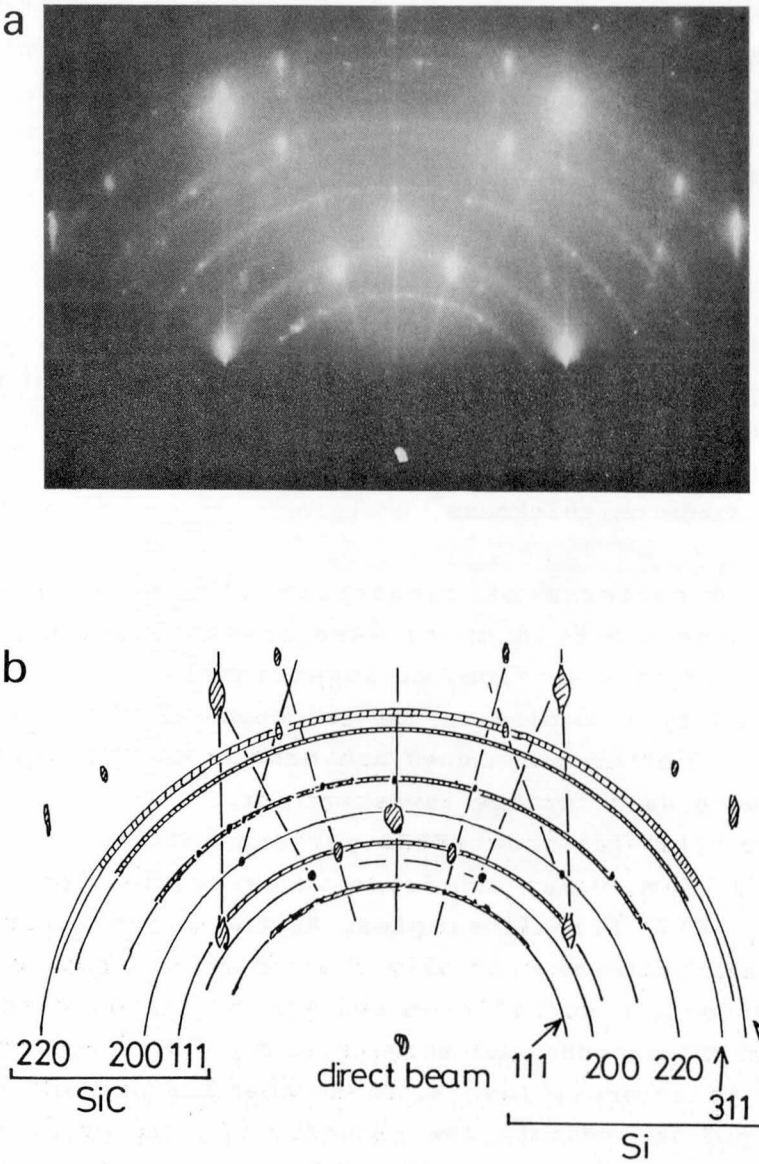

Fig.16 (a)RHHED pattern of a layer grown under the Si-rich condition. (b)Schematic explanation of (a). Solid arcs represent theoretically obtained Debye rings for Si and 3C-SiC. Observed patterns are drawn as shaded bands and spots.

susceptors were used, the flow rate of C_3H_8 must be decreased. Such a result indicates that graphite susceptors with a poor coating work as a carbon source. Surface morphology of the edge area was also affected by coating. Irrespective of the quality of coating, the surface in the edge part was rougher than that in the middle part. When in situ-coated susceptors were used, the area of such a part was wider. Carbon or some impurities which were contained in graphite were considered to affect the surface morphology. Even for epitaxial growth of Si whose typical growth temperature is lower than 1200°C, the prevention of contamination from susceptors are very important[8]. Since the growth temperature for SiC is very high, more solid and durable coating is demanded.

4-2. Dependence on thickness

In RHEED patterns of carbonized layers streaks due to stacking faults and twin spots were observed as described in Section 3-1. In this section, an investigation of the change in the crystallinity according to the thickness of the grown layers using RHEED and other techniques are mentioned. The grown layers on Si(100) were used for the investigation.

Figures 17(a)-(c) show RHEED patterns of the grown layers which were 0.15μm, 0.9μm and 5.4μm in thickness. The incidence azimuth was <011> for all samples. As the grown layers became thicker, RHEED patterns gradually changed from a spot pattern to a streak pattern. Kikuchi lines and Kikuchi bands were clearly observed and twin spots and streaks along <111>* disappeared in the case of thick grown layers. These changes in RHEED patterns are considered to indicate the reduction in the crystal defects which were observed in the carbonized layer. In other words, the crystallinity of the grown layer was improved as the film grew. To confirm the improvement of the crystallinity, channeling and X-ray diffraction techniques were utilized. The channeling spectra of Si atoms in the grown layers were obtained with 1MeV He^+. As shown in Fig.18, yields of backscattered ions decreased

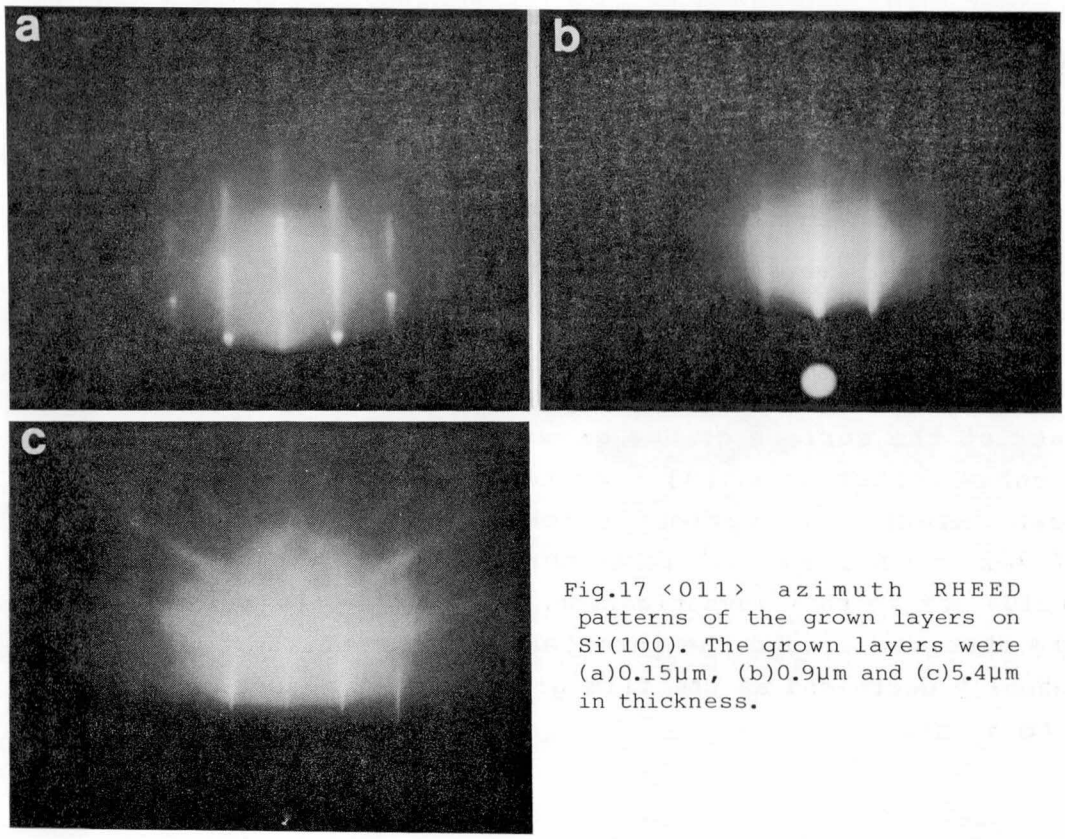

Fig.17 <011> azimuth RHEED patterns of the grown layers on Si(100). The grown layers were (a)0.15μm, (b)0.9μm and (c)5.4μm in thickness.

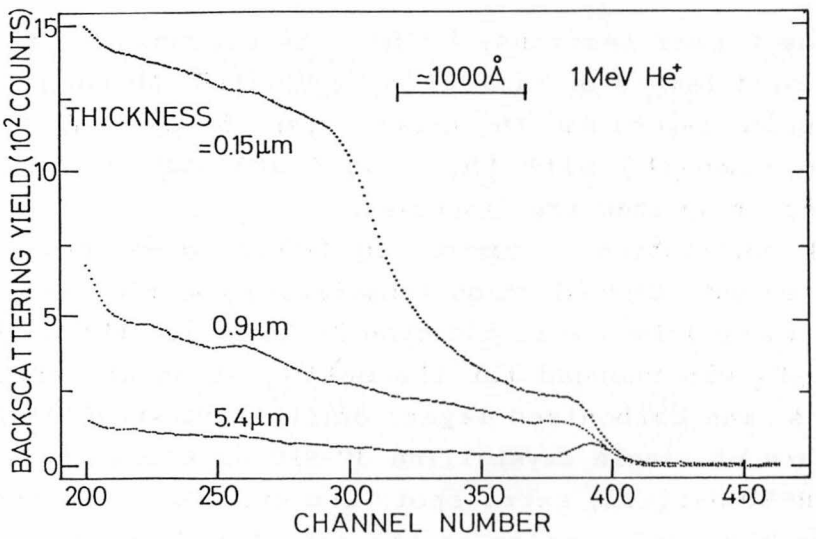

Fig.18 Channeling spectra of grown layers on Si(100).

as the film became thicker, which means improvement of crystallinity. In the case of X-ray diffraction, FWHM(full width at half maximum) of X-ray rocking curves decreased monotonously as the film became thicker as shown in Fig.19. These results obtained by both channeling and X-ray diffraction methods supported the improvement of the crystallinity of the grown layer by the increase of the film thickness.

In Section 3-1 an XTEM photograph of a CVD grown layer with a thickness of 100nm was shown. Many plane defects were observed as shown in Fig.11(a). The density of the plane defects was lower at the surface of the grown layer than at the interface. Recently Carter et al.[9] reported XTEM observation of 3C-SiC grown layers with various thicknesses. 3C-SiC was grown on Si(100) by a similar method to ours. They also obtained similar conclusions to this investigation. Stacking faults and microtwins were observed around the interface. They reported that defects gradually decreased as the film grew and such reduction continued up to 3-4μm.

5. Growth on Si(111), (110) and (211)

In the former sections, mainly the carbonized layers and the CVD grown layers on Si(100) were treated. In this section, the carbonized layers and the grown layers on Si(111), (110) and (211) are compared with those on (100) and the origin of differences among them are discussed.

RHEED observation of carbonized layers on various Si faces were carried out. Carbonization temperature and time were 1360°C and 2min. These values were the same as those for (100). The flow rate of C_3H_8 was changed for the optimization of carbonizing conditions. The carbonized layers on (111) substrates showed a spot pattern of single crystalline 3C-SiC as shown in Fig.20(a). In this RHEED pattern, extra-spots and streaks spreading along $\langle 111 \rangle^*$ are observed similar to the carbonized layers on (100). The carbonized layers on Si(111) were also considered to contain

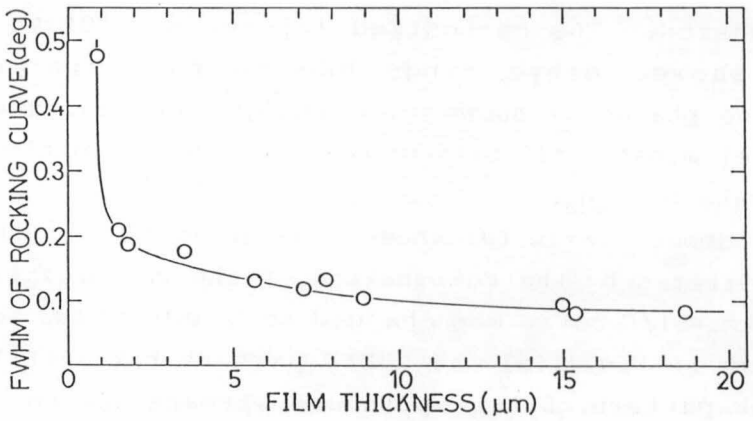

Fig.19 Film thickness dependence of FWHM of X-ray rocking curves of grown layers.

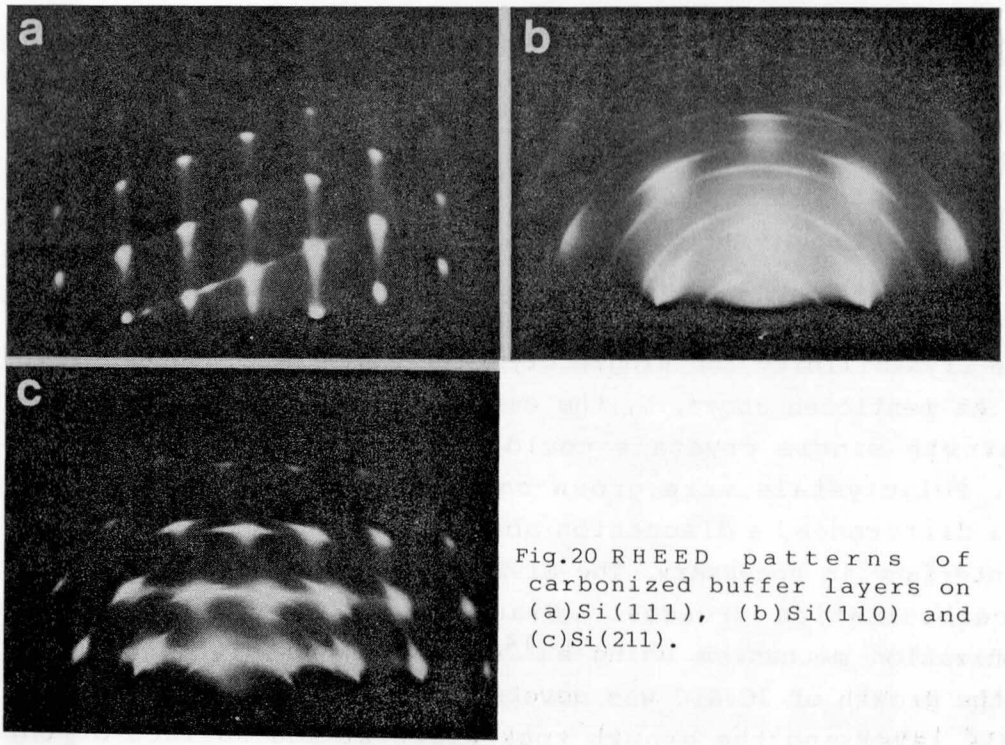

Fig.20 RHEED patterns of carbonized buffer layers on (a)Si(111), (b)Si(110) and (c)Si(211).

crystal defects due to the lattice mismatch or the difference in thermal expansion. The carbonized layers on (110) and (211) substrates showed Debye rings due to the existence of polycrystalline phases as shown in Figs.20(b) and (c). The rings could not be eliminated in spite of attempts for the optimization of the flow rate of C_3H_8.

3C-SiC of about 2μm in thickness was grown on Si(111), (110) and (211) substrates by the combination of the carbonization and the CVD growth. Si/C ratio was changed to be optimized for each face. As shown in Fig.21(a) the RHEED pattern for a (111) face was a streak pattern. Extra-spots and streaks due to crystal defects disappeared. Similar to the case of (100) mentioned in Section 4-2, the crystallinity of the grown layers on (111) was improved as the film became thicker. In contrast with (100) and (111), the grown layers on (110) and (211) showed no significant improvement in the crystallinity due to the increase of the thickness. As shown in Figs.21(b) and (c), grown layers on the (110) and (211) substrates gave extra-spots and Debye-rings in RHEED patterns. The surfaces of the grown layers on (110) and (211) substrates were very rough as shown in Figs.22(a) and (b). The optimization of the Si/C ratio was of no use for improvement of crystallinity and surface flatness. The crystallinity of the carbonized layers on (110) and (211) was considered to be too bad in the crystallinity for single crystal growth by subsequent CVD.

As mentioned above, by the carbonization and the subsequent CVD growth single crystals could be grown only on (100) and (111). Polycrystals were grown on (110) and (211). To explain such a difference, a discussion about the formation of the Si-SiC interface is necessary. The Si-SiC interface is formed during the carbonization process. Graul et al. investigated the carbonization mechanism using a ^{14}C tracer method and concluded that the growth of 3C-SiC was governed by diffusion of Si through the SiC layer and the growth took place at the surface of the sample[10]. Based on their conclusion, the initial stage of the carbonization was assumed to be composed of two steps as follows. [step 1] Growth of the first layer: Decomposed C_3H_8 molecules

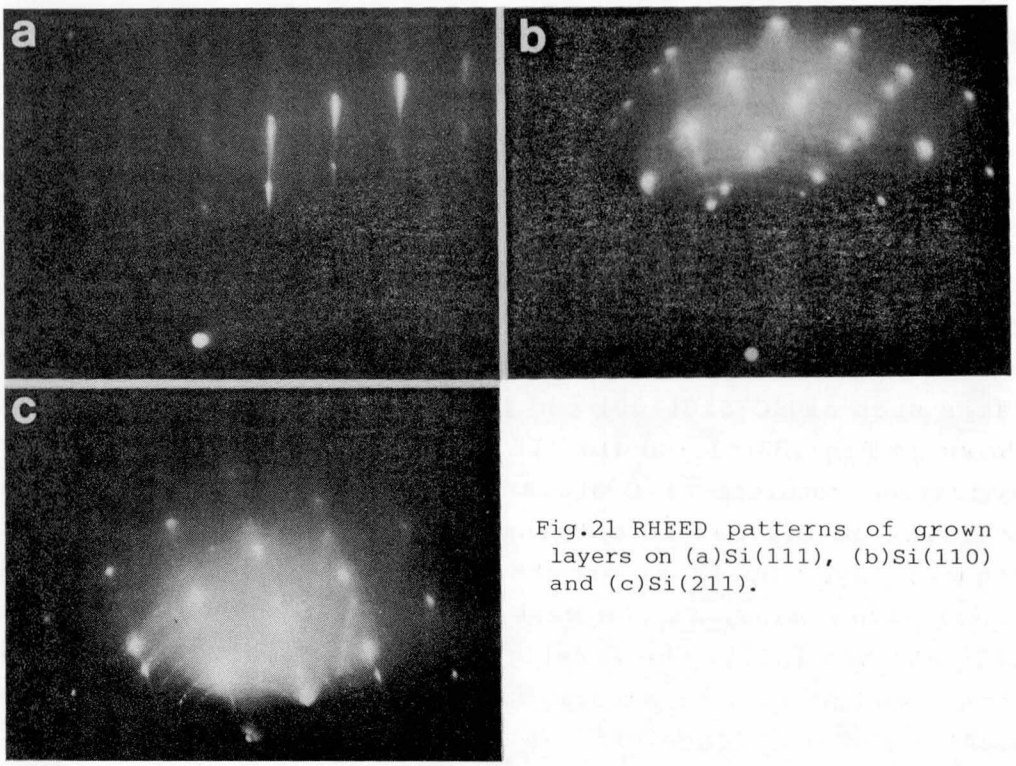

Fig.21 RHEED patterns of grown layers on (a)Si(111), (b)Si(110) and (c)Si(211).

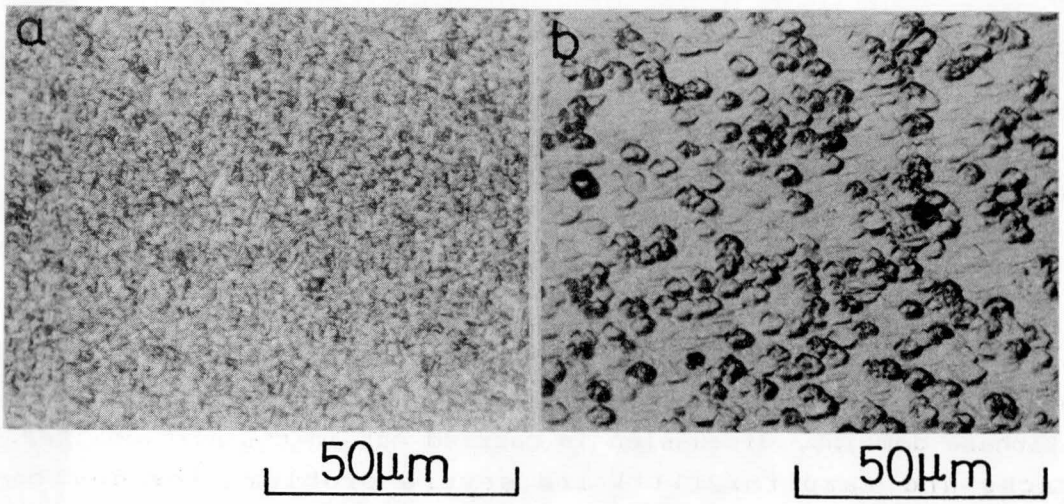

Fig.22 Nomarski microphotographs of surface morphology of the grown layers on (a)Si(110) and (b)Si(211).

adhere to the Si surface, and C atoms of a monoatomic layer cover the Si surface. [step 2] Subsequent growth: 3C-SiC grows at the surface of the carbonized Si substarate consuming out-diffused Si atoms and gaseous C_3H_8.

The step 1 of this assumption means that the first grown layer consists of C atoms only. Figures 23, 24(a) and 24(c) show the arrangements of the atoms around the ideal Si-SiC interface for various orientations. To make the discussion simple, the large lattice mismatch of about 20% between Si and 3C-SiC is neglected in Figs.23 and 24. The ideal first grown layer of polar surfaces such as 3C-SiC(100) and (111) should have only C atoms as shown in Figs.23(a) and (b). If the first grown layer by the carbonization consists of C atoms only as assumed above, single crystalline 3C-SiC can be obtained on (100) and (111) faces by subsequent layer-by-layer growth in the order of Si, C, Si and C. On the other hand, in the case of nonpolar surfaces such as 3C-SiC(110) and (211), the first grown layer should be composed of both C and Si atoms to form the 3C-SiC lattice as shown in Figs.24(a) and (c). Hence, if the first layer is a carbon layer as assumed, single crystalline 3C-SiC cannot be obtained by the subsequent growth on (110) and (211) faces. By assuming that the first grown layer by the carbonization consists of carbon atoms only, the difference in the crystallinity of the carbonized layers due to the crystal faces was explained. This assumption is important for the discussion of the origin of antiphase domains in Chapter III.

Thus, by the combination of carbonization and subsequent CVD growth single crystalline 3C-SiC was obtained on Si(100) and (111) substrates. However, problems remain in the grown layers on these substrates. For (100) antiphase domains and for (111) warp and cracks are major problems. Concerning the elimination of antiphase domains, discussion is carried out in the next chapter. Cracks and warp for (111) are severe problems for device application. An example of cracks is shown in Fig.25. The cracks were not observed during the grown layers were thinner than 10μm. While the grown layers were thin, the warp or wavy surfaces were

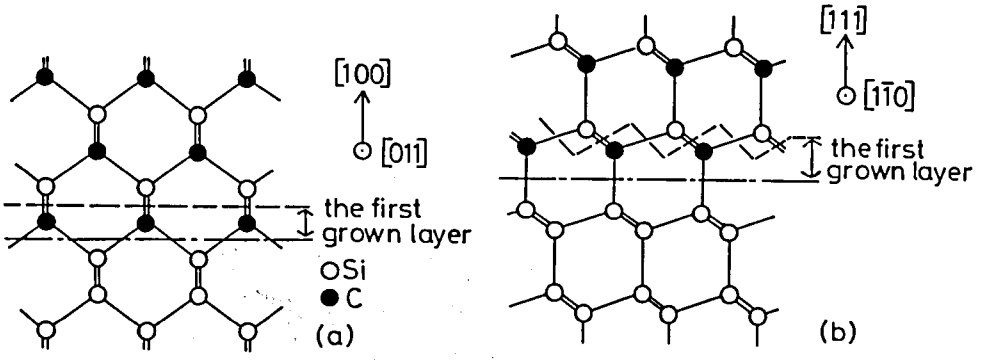

Fig.23 Ideal atomic arrangements of interfaces between Si and SiC. (a)SiC/Si(100) and (b)SiC/Si(111).

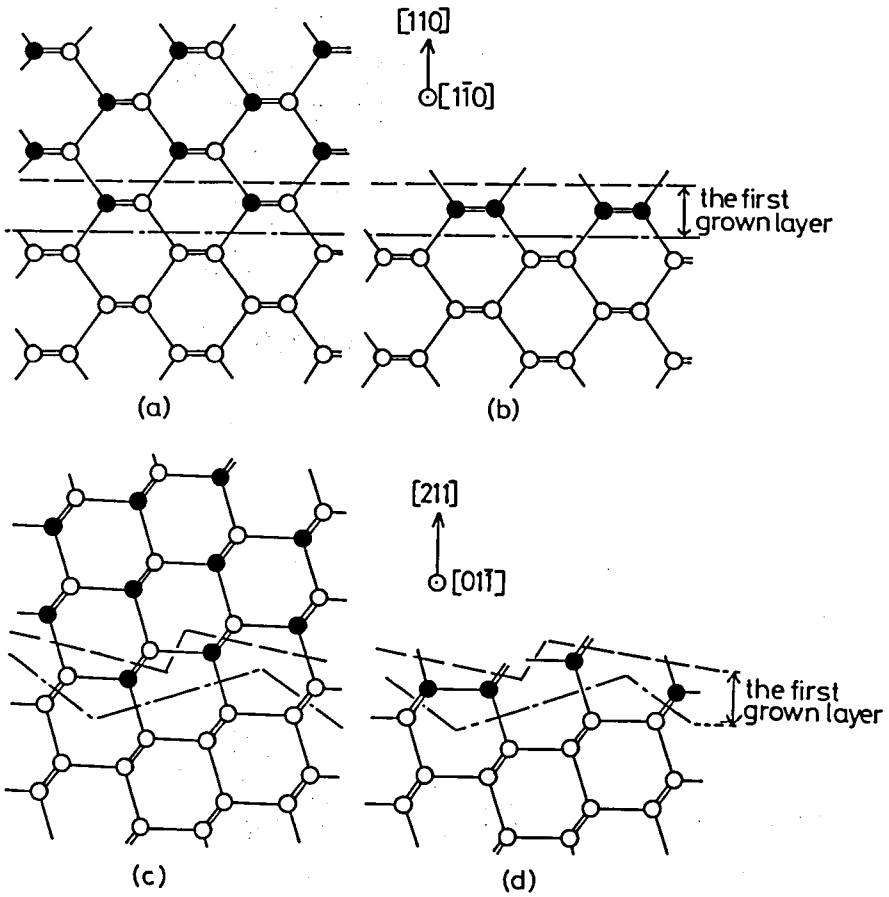

Fig.24 Atomic arrangements of interfaces between Si and SiC. Ideal cases: (a)SiC/Si(110) and (c)SiC/Si(211). The first grown carbon layer formed by carbonization on (b)Si(110) and (d)Si(211).

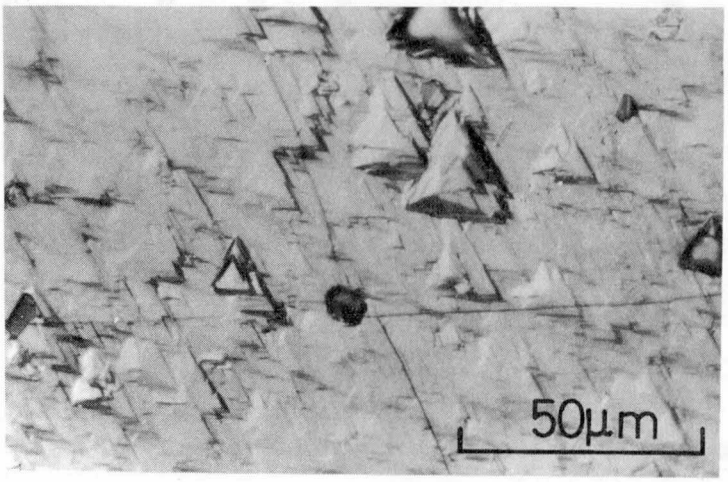

Fig.25 Cracks observed on a grown layer on Si(111).

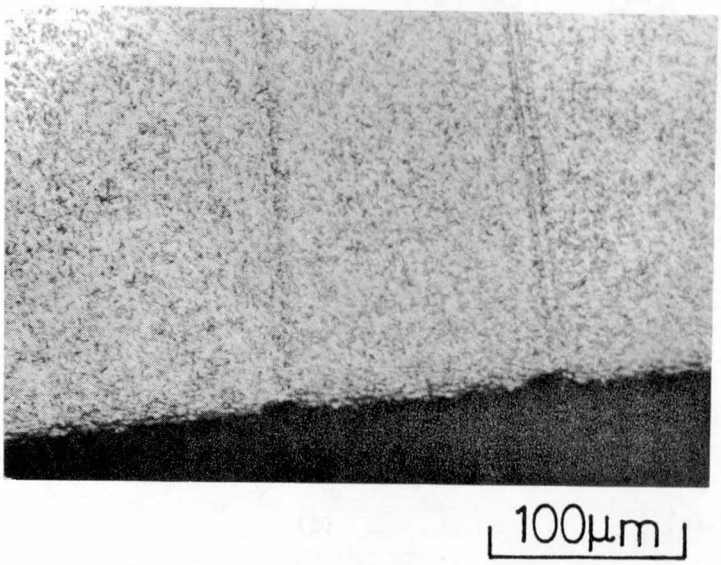

Fig.26 Slip lines observed on a grown layer on Si(100).

observed. There are two considerable origins of the warp such as the lattice mismatch and the difference in the thermal expansion coefficient. Suzuki[11] reported that the warp can be observed during growth. Hence, the main factor which gives rise to the warp and cracks are considered to be stress due to the difference in lattice constants. While the film is thin enough, the stress results in the warp. And when the thickness exceeds a certain limit, the stress gives rise to cracks.

6. Attempt for low temperature growth

In this section a trial to reduce growth temperature is mentioned. The ordinary growth temperature of 3C-SiC on Si substrates is 1350°C. This temperature is rather higher than process temperatures which are necessary for the fabrication of practical Si devices. High growth temperatures sometimes give rise to problems as follows. Contamination from the inside of a growth system easily takes place. As an example of such contamination the supply of carbon by the susceptor with poor coating was mentioned in Section 4-1. Since the growth temperature is close to 1420°C of the melting point of Si, deterioration of Si substrates in crystallinity is anticipated. In truth, slip lines are always observed after the HCl etching and the growth. An example of slip lines are shown in Fig.26. Flexibility in the fabrication process of devices is damaged by the high growth temperature.

In addition to the problems mentioned above, the diffusion of impurities due to high process temperature is an important problem in the case of growth of Si. Therefore, many attempts have been carried out to reduce growth temperature of Si. The selection of source gas is important to reduce the growth temperature of Si. A typical growth temperature of Si using a $SiCl_4$-H_2 system is 1150-1250°C. By using SiH_4, the growth temperature was reduced to 950-1050°C[12]. Recently growth at 700°C using Si_2H_6 was reported[13].

In this work, growth of 3C-SiC using C_2H_2 as a carbon source was carried out with the aim of the reduction in growth temperature. C_2H_2 was diluted with H_2. Si(100) well-oriented substrates were used. The crystal growth procedure was the same as those mentioned in Section 2. The carbonization temperature was fixed at 1360°C. The optimization of carbonizing conditions was carried out by varying the flow rate of C_2H_2. The growth temperatures were changed in the range of 1150-1350°C.

First, the growth rate was fixed at about 1.8μm/hr and the growth temperature was reduced. This growth rate was a typical one for CVD growth using C_3H_8 at 1350°C. Figure 27 shows the surface morphology and the RHEED patterns of 3C-SiC grown at various temperatures. The growth time was 1hr. The Si/C ratio was optimized at each growth temperature. Single crystalline 3C-SiC was obtained at 1350°C and 1300°C. The surface morphology was almost similar to that obtained using C_3H_8.* In the case of 1250°C twin spots were slightly observed in the RHEED pattern. When the growth temperature was reduced again, ringlike spots(1200°C) and complete ring(1100°C) patterns were observed. In other words, under 1250°C the grown layers contained twinning or polycrystals. The surface morphology also changed from a single-crystal-like orderly pattern to a polycrystal-like random pattern as the growth temperature reduced.

(*A typical surface morphology of 3C-SiC grown with C_3H_8 on similar substrates is shown in Section III-2-1.)

As growth temperatures are reduced, surface migration becomes inactive. In order to make up for the insufficiency of migration, the growth rate was reduced. The growth time was prolonged to keep comparable thickness. RHEED patterns of the grown layers are shown in Fig.28. At 1250°C and 1200°C single crystals were obtained at growth rates of 0.72μm/hr and 0.54μm/hr, respectively. Surface morphology changed from one with a random feature to the similar one obtained at 1350°C by the reduction in the growth rate. At 1150°C the growth rate was reduced to 0.45μm/hr. The RHEED pattern of this grown layer in Fig.28(c) showed an improvement in the crystallinity compared

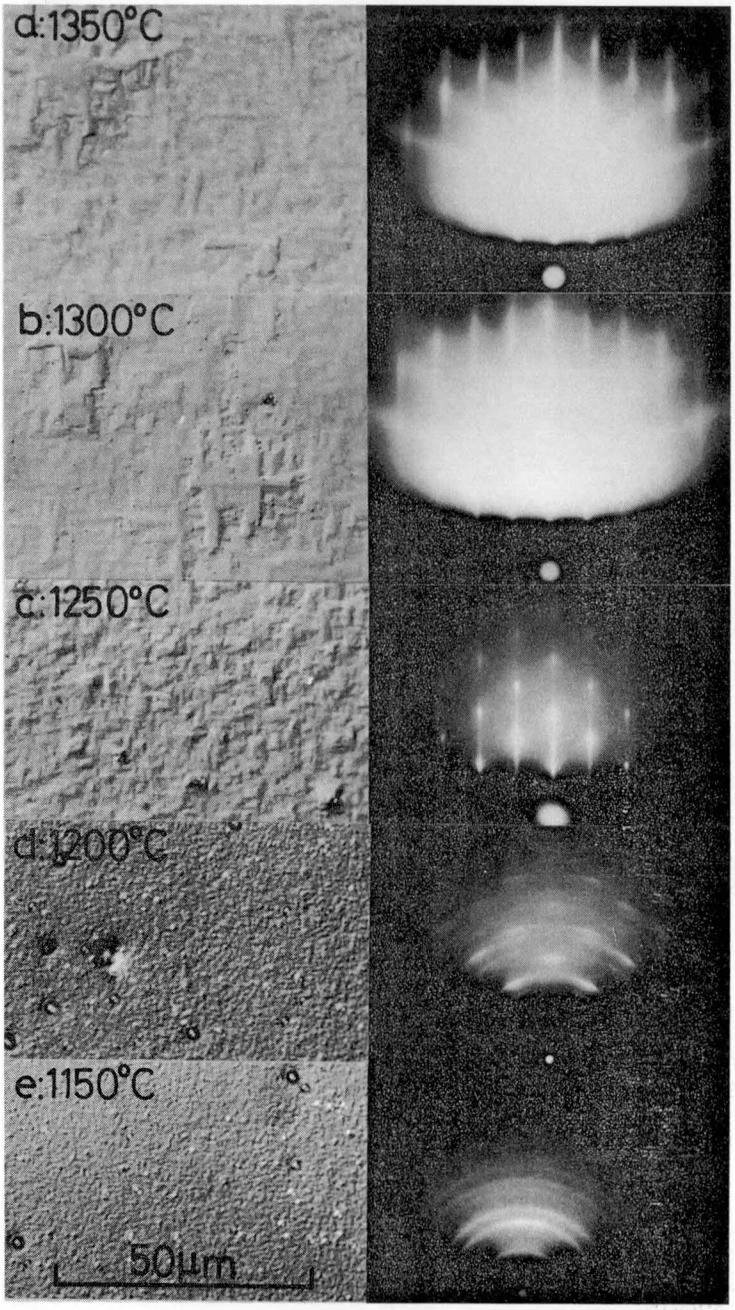

Fig.27 Nomarski microphotographs of surface morphology and [011] azimuth RHEED patterns of 3C-SiC grown using C_2H_2. Growth temperatures were (a)1350°C, (b)1300°C, (c)1250°C, (d)1200°C and (e)1150°C. Growth rate was about 1.8μm/hr.

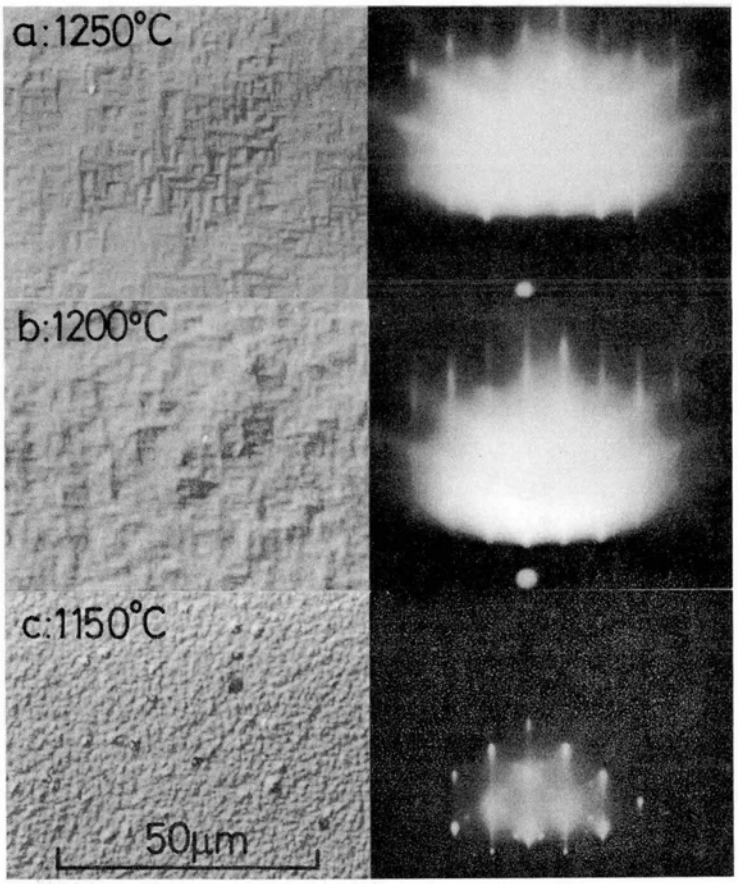

Fig.28 Nomarski microphotographs of the surface morphology and RHEED patterns of 3C-SiC grown using C_2H_2. By the reduction in growth rates, crystallinity was improved compared with Fig.27. Growth temperatures and growth rates were (a)1250°C and 0.72μm/hr, (b)1200°C and 0.54μm/hr and (c)1150°C and 0.54μm/hr, respectively.

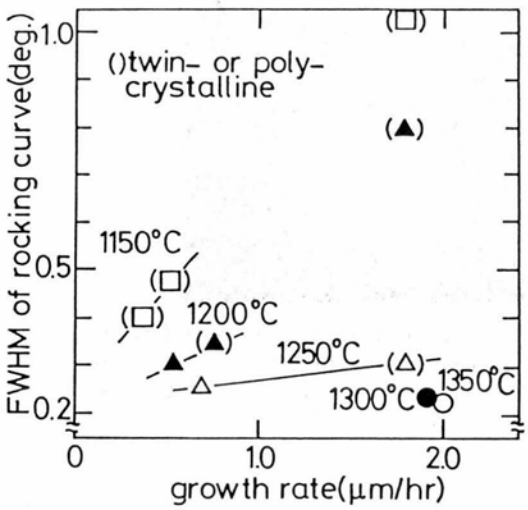

Fig.29 Growth rate dependence of FWHM of x-ray rocking curves of grown layers.

with Fig.27(e). Debye-rings disappeared and extra-spots were reduced. However, twin-spots remains slightly. Though optimization of the Si/C ratio was carried out, twin-spots did not disappear. Surface morphology in Fig.28(c) still remains a random feature. Thus, by the reduction in the growth rate single crystals were obtained at low temperatures of 1250°C and 1200°C.

A further evaluation of the grown layers prepared with C_2H_2 was carried out. The FWHM of X-ray rocking curves of these grown layers are shown in Fig.29. When the growth rate was fixed at about 1.8μm/hr, as the growth temperature was reduced, the FWHM of rocking curves became wider. And by the reduction in the growth rate, the FWHM became narrower. These results agree with the change in the crystallinity observed by RHEED technique. However, in spite that the samples grown at 1250°C and 1200°C showed single crystalline streak patterns by RHEED observation, their FWHM of X-ray rocking curves were wider than those of the samples grown at over 1300°C. This fact indicates that the lack of migration effect due to low growth temperature was not sufficiently made up for by the reduction in the growth rate.

The characteristics of Au-SiC Schottky barriers were evaluated using the samples which showed single crystalline features in RHEED observation. Figure 30 shows an example of the current-voltage characteristics of the Schottky diodes. The layers grown at low temperatures showed worse rectification than those grown at high temperatures. Figure 31 shows a variation of barrier height(ϕ_{bn}) and ideal factor *n*. As the growth temperature was reduced, the barrier height became lower and ideal factor *n* became larger. Such variations are considered to support the change in the crystallinity due to growth temperature observed as the change of FWHM of X-ray rocking curves. However, electron mobility and electron concentration obtained by the van der Pauw measurement showed no meaningful difference. Electron mobility is often governed not only by crystallinity but also by ionized impurity scattering and some other scattering mechanisms. Hence, the temperature dependence of electron mobility should be investigated to discuss the effects of crystallinity upon the

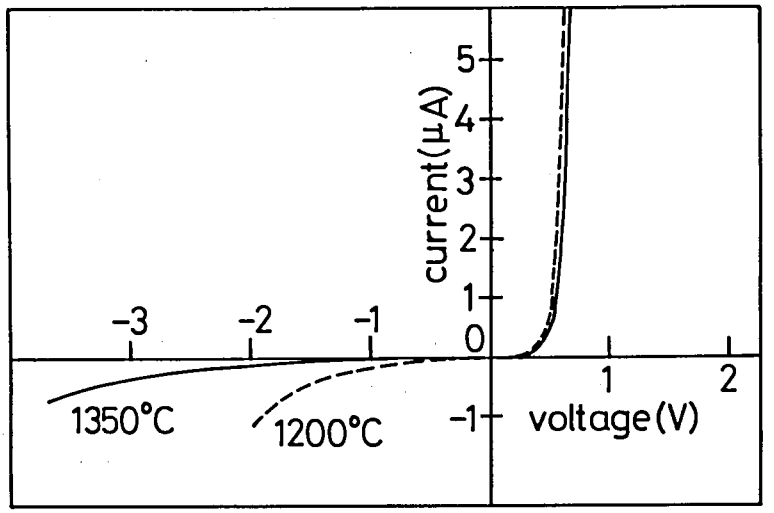

Fig.30 Example of rectification of Au-3C-SiC Schottky barrier. 3C-SiC grown at low temperatures(<1250°C) showed poor rectification.

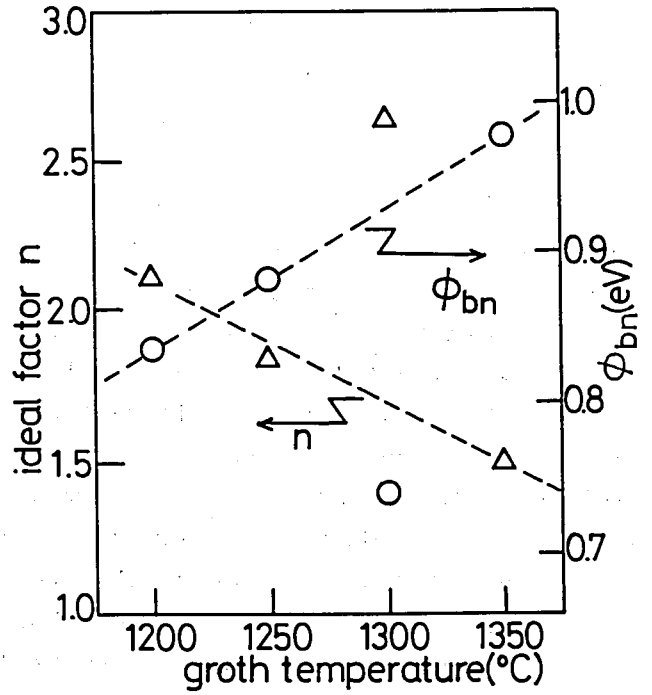

Fig.31 Growth temperature dependence of *n* value and barrier height(ϕ_{bn}) of Au-3C-SiC Schottky barrier.

electron mobility.

*Note: Recently the conversion of C_2H_2 into C_2H_4 under a H_2 ambience in cylinders was found[14]. The same phenomenon was considered to take place in the used cylinders for this investigation. Because, the moderate Si/C ratio always varied after the replacement of the cylinders of C_2H_2. In other words, the used carbon source was a mixture of C_2H_2 and C_2H_4. Therefore, the Si/C ratio was not discussed in detail in this section.

7. Summary

Characterization of carbonized layers was carried out. By RHEED observation the carbonized layers grown under optimized conditions were found to be single crystalline 3C-SiC. However, they contained crystal defects such as stacking faults and twinning. The density of these defects in CVD grown layers was reduced as the film grew, which was supported by RHEED, X-ray diffraction, channeling measurement and XTEM.

Single crystal growth of the 3C-SiC polar faces such as (100) and (111) was successful. However, the growth of nonpolar faces such as (110) and (211) was unsuccessful, which was explained by assuming the first grown layer by the carbonization to be a carbon layer. The grown layer on (111) has a severe problem of cracks and warp.

Temperature for single-crystal growth could be reduced to 1200°C by the reduction in growth rate. The reduction in the growth rate was effective to make up for the insufficiency of migration effect. However, crystals grown at low temperatures were inferior to those grown at high temperatures in crystallinity. If further reduction in the growth temperature will be attempted, some innovations which enhance migration may be necessary.

By considering all results mentioned in this section the

following factors which are necessary to obtain "good crystals" are selected. The current best substrate is Si(100). To improve crystallinity the grown layers had better be thicker than several microns. The carbonizing condition and the Si/C ratio must be optimized and the growth should be carried out at 1350°C. The growth of 3C-SiC on Si for the investigation of the following chapters was carried out in accordance with this guideline.

References

[1] F.C.Everstyen, P.J.W.Severn, C.H.J.v.d.Brekel and H.L.Peek, J. Electrochem. Soc. 117(1970) 925.

[2] I.Tani, *Nagaregaku(Hydrodynamics)*, (Iwanami, Tokyo, 1967), p.131, in Japanese.

[3] H.Suhara, Master Thesis, Faculty of Engineering, Kyoto University, 1983.

[4] P.B.Hirsch, A.Howie, R.B.Nicholson, D.W.Pashley and M.J.Whelan, Electron Microscopy of Thin Crystals, (Butterworths, London, 1965), Chapter 6.

[5] M.Plutton, *Surface Physics*, (Oxford Univ. Press, Oxford, 1975), Chapter 3.

[6] C.J.Dell'Oca, J. Electrochem. Soc. 120(1973) 1225.

[7] T.Ito, T.Inuzuka, *Kessyou No Hyouka(Characterization of Crystals)*, (Corona, Tokyo, 1982), p.107, in Japanese.

[8] T.Ohmi, S.Kuroiwa, S.Yoshitake, H.Iwabuchi, G.Sato and J.Murota, Extended Abstr. 19th Conf. Solid State Devices and Materials, Tokyo, 1987(Business Center for Academic Societies Japan, Tokyo, 1987) p.239.

[9] C.H.Carter, Jr., R.F.Davis and S.R.Nutt, J. Mater. Res., 1(1986) 811.

[10] J.Graul and E.Wagner, Appl. Phys. Lett. 21(1972) 67.

[11] A.Suzuki, private communication.

[12] C.W.Pearce, *VLSI Technology*, (McGraw-Hill, Auckland, 1983) edited by S.M.Sze, Chapter 2.

[13] F.Mieno, Y.Furumura and M.Maeda, Extended Abstr. 18th Int.

Conf. Solid State Devices and Materials, Tokyo, 1986(Business Center for Academic Societies Japan, Tokyo, 1986) p.49.
[14] H.Shiomi, private communication.